On the compression behaviour of $(Ti_{0.5},V_{0.5})_2AlC$ and $(Ti_{0.5},Nb_{0.5})_2AlC$ to quasi-hydrostatic pressures above 50 GPa

2007 J. Phys.: Condens. Matter 19 246215

(http://iopscience.iop.org/0953-8984/19/24/246215)

IOP PUBLISHING JOURNAL OF PHYSICS: CONDENSED MATTER

J. Phys.: Condens. Matter **19** (2007) 246215 (8pp) doi:10.1088/0953-8984/19/24/246215

On the compression behaviour of $(Ti_{0.5}, V_{0.5})_2AlC$ and $(Ti_{0.5}, Nb_{0.5})_2AlC$ to quasi-hydrostatic pressures above 50 GPa

Bouchaib Manoun[1,2,4], **Fuxiang Zhang**[1], **Surendra K Saxena**[1], **Surojit Gupta**[3] **and Michel W Barsoum**[3]

[1] Center for Study of Matter at Extreme Conditions (CeSMEC), Florida International University, VH-140, University Park, Miami, FL 33199, USA
[2] Laboratoire de Physico-Chimie des Matériaux, Département de Chimie, FST Errachidia, University Moulay Ismail, Morocco
[3] Department of Materials Science and Engineering, Drexel University, Philadelphia, PA 19104, USA

E-mail: manounb@fiu.edu

Received 27 March 2007, in final form 24 April 2007
Published 24 May 2007
Online at stacks.iop.org/JPhysCM/19/246215

Abstract

Using a synchrotron x-ray radiation source and a diamond anvil cell we measured the functional dependences of the lattice parameters of $(Ti_{0.5},V_{0.5})_2AlC$ and $(Ti_{0.5},Nb_{0.5})_2AlC$ to quasi-hydrostatic pressure of the order of 50 GPa. Like for other solids in this family of layered ternary carbides and nitrides, the bulk moduli ($\approx$183 GPa) are high and no phase transformations were observed. The bulk moduli of the solid solution compositions were lower than those of the end members. The effect was much more dramatic when Ti replaced Nb in Nb_2AlC than when it replaced V in V_2AlC. In the former case the modulus drops by 13% from 209 GPa, with the softening coming almost exclusively from the *c*-axis. This somewhat surprising result is ascribed to the corrugation of the Ti–Nb planes in $(Ti_{0.5}, Nb_{0.5})_2AlC$. When Ti replaced V in V_2AlC the drop in modulus was 8%.

(Some figures in this article are in colour only in the electronic version)

1. Introduction

The $M_{n+1}AX_n$ (MAX) compounds, where $n = 1$, 2 or 3, M is an early transition metal, A is an A-group (mostly IIIA and IVA) element, and X is C or N, have been studied extensively these last few years [1–5]. These carbides adopt a hexagonal crystal structure consisting of layers of edge sharing MC_6 octahedra interleaved with square-planar A layers. The edge sharing TiC_6

[4] Author to whom any correspondence should be addressed.

octahedra are identical to those found in the rock salt structure of the corresponding binary carbides, MX [6].

Among the M_2AX phases, Ti_2AlC has been widely studied due to its commercial availability, superb oxidation resistance even under severe thermal cycling [7]. It is also a good thermal and electrical conductor. Its density is comparable to Ti, but its elastic moduli are roughly three times as high. It is also damage tolerant and thermal shock resistant. It is relatively soft (Vickers hardness ≈ 2 GPa) and most readily machinable [8]. This combination of properties derives partially from the metallic nature of the bonding, partially from the layered nature of the structure and partially from the fact that basal plane dislocations are mobile at all temperatures. We have also recently shown that the attenuation of sound waves in Ti_2AlC was higher than many woods and comparable to some polymers [9, 10].

Over the last few years a concerted effort has been made to try to understand the relationship between MAX phase chemistries and their mechanical and elastic properties. Most germane to this paper are the bulk moduli. Recently Manoun *et al* [11–15] reported on the compression behaviour of M_2AlC (M = Ti, V, Cr, Nb and Ta) [11], $Ti_3Si_{0.5}Ge_{0.5}C_2$ [12], Zr_2InC [13], Ti_4AlN_3 [14] and Ta_4AlC_3 [15]. In all cases, like in Ti_3SiC_2 [16], no phase transitions were observed up to pressures of the order of 55 GPa. The isothermal bulk moduli, K_0, of these compounds, varied from a high of 261 GPa for Ta_4AlC_3 [15], to a low of 127 GPa for Zr_2InC [13]. For the most part, the relative shrinkage along the *c*-direction with pressure was greater than along the *a*-direction. The exceptions were Cr_2AlC [11], Nb_2AsC [17] and Nb_2AlC [11]. The Ta-containing phases were unique in that the shrinkages along both directions were quite similar [11, 15].

Recently we have also explored the effects of solid solutions on the X-sites and A-sites. For example, it has been shown that replacing the C by N in Ti_2AlC results in a decrease in bulk moduli [18]. Replacing Ge by Si in Ti_3GeC_2, on the other hand, does not affect K_0 greatly [19]. Interestingly, only the substitutions on the X-sites result in significant hardening [8]. This paper represents our first attempt to explore the effects of solid solution substitutions on the M-sites on K_0. The excellent miscibility of the solid solution series on the M-sites in M_2AlC (M = Ti, V, Nb and Cr) systems was experimentally confirmed by Schuster and co-workers in 1980 [20]. More recently, Salama *et al* synthesized $(Ti_{0.5}, Nb_{0.5})_2AlC$ and investigated its mechanical properties and observed no solid solution hardening effects [21].

Sun *et al* [22–24] carried out *ab initio* total energy calculations using the projector augmented wave method on M_2AlC (M = Ti, V, Cr, Ta and Nb) and $(Ti,V)_2AlC$ [22]. The K_0 values—calculated from theory (see table 1) were predicted to increase by 19% and 24%, respectively, as Ti was substituted by V or Nb.

The combination of easy machinability, relative low densities (of some of the phases) and high elastic constants, together with the possibility of extremely high damping [25, 26] is one that to date had not been possible. Thus one motivation for this work was to identify compositions of potential technological interest. The second motivation was to directly measure, for the first time, K_0 of $(Ti_{0.5},Nb_{0.5})_2AlC$ and $(Ti_{0.5},V_{0.5})_2AlC$—henceforth referred as TiNbAlC and TiVAlC, respectively—and compare them to the end members compositions measured previously, viz. Ti_2AlC, V_2AlC and Nb_2AlC. We were also interested in exploring the stability of these phases at high pressures.

2. Experimental details

The processing details of the TiVAlC samples were described elsewhere [27]. In short, Ti, V, Al and C powders were mixed in the stoichiometric composition and sealed in borosilicate glass tubes under a mechanical vacuum. The tubes were heated to 650 °C for 10 h, which resulted in their collapse. The collapsed tubes were placed in a hot isostatic press (HIP), which was

Table 1. Ambient pressure lattice parameters and unit cell volumes of the M_2AlC compounds and solid solutions measured herein. Also listed are previous results. The space group adopted for all phases is $P6_3/mmc$. References [6, 20] and [21] are experimental measurements. References [23] and [34] are theoretical; reference [33] is both.

M_2AlC	V_2AlC	TiVAlC	Ti_2AlC	TiNbAlC	Nb_2AlC
a (Å)	2.914 ± 0.003	2.98 ± 0.01	3.065 ± 0.004	3.08 ± 0.01	3.103 ± 0.004
	2.909[b]	2.979[g]	3.058[a]	3.077[a]	3.106[a]
	2.925[d]	2.975[b]	3.052[b]		3.107[e]
			3.062[d]		3.129[f]
c (Å)	13.19 ± 0.03	13.42 ± 0.04	13.71 ± 0.03	13.80 ± 0.04	13.93 ± 0.03
	13.127[b]	13.471[g]	13.624[a]	13.79[a]	13.888[a]
	13.105[d]	13.393[b]	13.64[b]		13.888[e]
			13.673[d]		13.895[f]
V_0 (Å)^3	97.0 ± 0.7	102.8 ± 0.6	111.6 ± 0.6	113.4 ± 0.7	116.2 ± 0.7

[a] Reference [33].
[b] Reference [20].
[c] Reference [6].
[d] Reference [23].
[e] Reference [21].
[f] Reference [34].
[g] Reference [22].

heated at 10 °C min^{-1} to 650 °C, followed by a rate of 2 °C min^{-1} to 750 °C. The chamber was then pressurized to 40 MPa using Ar; once pressurized, the heating continued at 10 °C min^{-1} to 1600 °C. The samples were held at that temperature for 8 h under a pressure of ≈70 MPa. A similar procedure was employed to fabricate the TiNbAlC samples [21]. Here again the samples were held at 1600 °C for 8 h at ≈100 MPa.

The x-ray diffraction, XRD, patterns for TiNbAlC and TiVAlC were collected using a $\lambda = 0.496$ Å of a monochromatic beam focused down to a 35 μm spot size, collected at CHESS (Cornell Univ., Ithaca, NY). Diffraction rings were recorded between $2\theta = 1°$ and 35° using an image plate.

Measurements were conducted at room temperature; powdered samples were pressurized using a gasketed Diamond Anvil Cell (DAC) with a 300 to 400 μm culet. A 250 μm initial thickness rhenium gasket, was indented to about 40–60 μm.

The stress state of a sample compressed in a DAC can become highly nonhydrostatic if the material is hard and has low compressibility like the MAX phases. However, it has been shown that the sample pressure can be rendered nearly hydrostatic by using a large volume of a low shear strength material as a pressure-transmitting medium. We have repeatedly shown that Al—with its low shear modulus and lack of phase transitions—was a good pressure-transmitting medium [11–15, 18, 19, 28, 29]. Another advantage of Al is the fact that its pressure–volume relationship is well established [30]. In this work, powdered samples were placed between two 15 μm thick Al foils, before packing them in the 100–150 μm hole in the Re gasket.

The FIT2D software [31, 32] was employed to convert the image plate records into 2θ's and intensities. The a and c lattice cell parameters were determined using least squares refinement on individually fitted peaks.

3. Results and discussion

All the major peaks in the XRD patterns of studied phases were assigned to the hexagonal structure with the space group $P6_3/mmc$. Figure 1 shows the indexed XRD pattern for

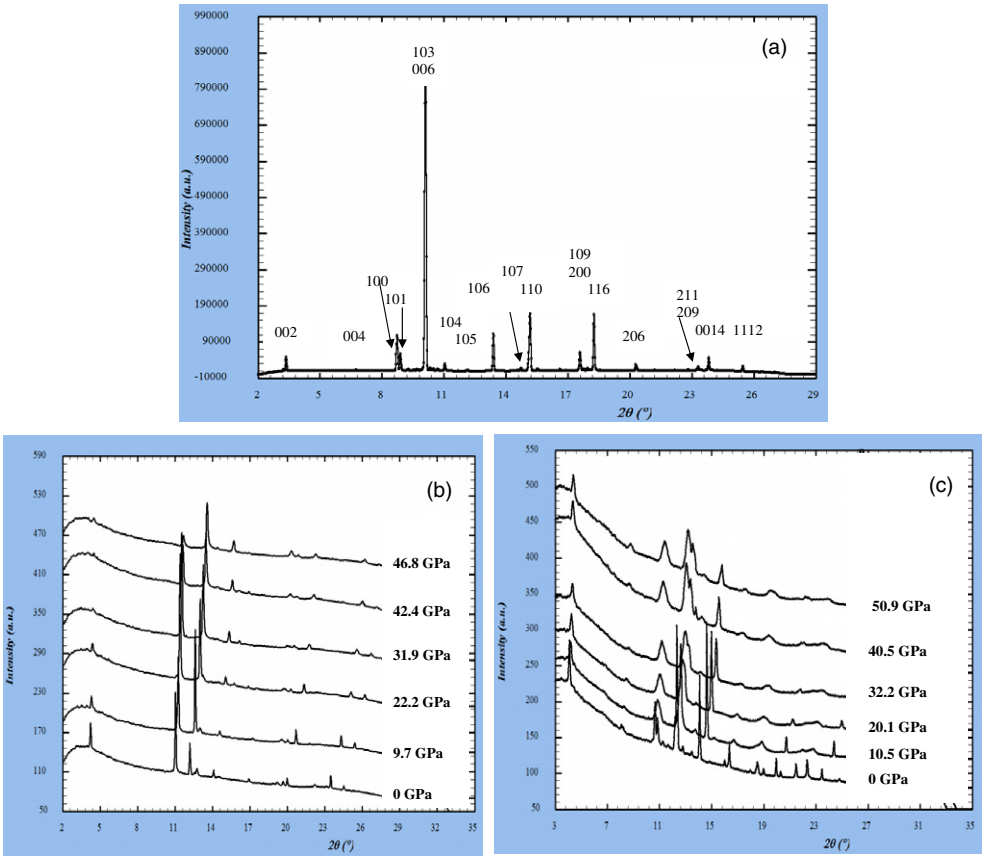

Figure 1. (a) X-ray diffraction pattern of TiNbAlC taken at room conditions, ($\lambda = 0.4066$ Å). (b) Functional dependence of high-pressure XRD spectra for TiVAlC on quasi-hydrostatic pressure, P ($\lambda = 0.496$ Å). (c) Functional dependence of high-pressure XRD spectra for TiNbAlC on P ($\lambda = 0.496$ Å). In both cases, upon compression, most peaks remain visible until the highest pressures are reached. With increasing P, the peaks become broader, lose intensity, and some merge together. No extra peaks appear in the patterns up to about 50 GPa.

NbTiAlC. This spectrum was recorded, using a wavelength of 0.4066 Å, at HPCAT (APS, Chicago). In general the agreement between the unit cell parameters measured in this study, those previously reported [6, 20, 21, 33, 34], and those predicted from the *ab initio* calculations [22, 23] is acceptable (table 1). Typical high-pressure XRD spectra of TiVAlC (figure 1(b)) and TiNbAlC (figure 1(c)) recorded under quasi-hydrostatic pressure show that for both samples, most peaks remain visible until the highest pressures reached. With increasing pressure, however, the peaks become broader, lose intensity, and some merge together. No extra peaks appear in the patterns up to about 50 GPa, which indicates the stability of these phases under quasi-hydrostatic pressure and is in line with previous work. As noted above, to date all MAX phases have been stable up to the highest pressures reached (≈50 GPa).

Figure 2(a) plots the variations in a/a_0 and c/c_0 versus applied quasi-hydrostatic pressure P. (The subscripts refer to the values of a and c when $P = 1$ atm.) A second order polynomial least square fits resulted in the coefficients listed in table 2. Note that for both quaternaries the contraction along the c-direction is greater than along the a-direction. Interestingly, Ti_2AlC

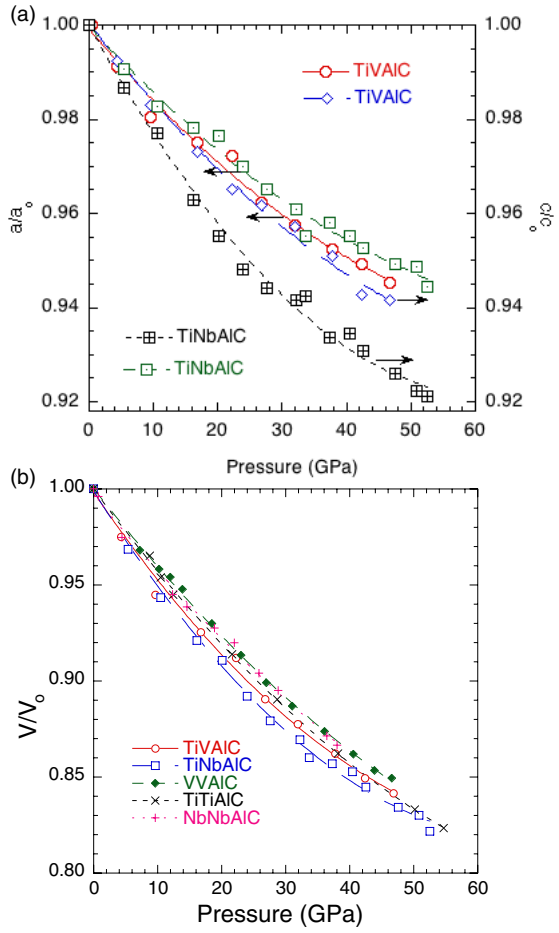

Figure 2. Pressure dependences of, (a) the a/a_0 and c/c_0 and, (b) V/V_0 for TiVAlC and TiNbAlC. The lines are least square fits of the data points. Also included in (b) are the results for the end members taken from [11].

Table 2. Relative lattice parameter changes with pressure, P. P_0 defines the units used and is equal to 1 GPa. The correlation coefficient values in all cases were greater than 0.99.

M_2AlC	Max pressure (GPa)	$a/a_0 = 1 + \beta P/P_0 + \gamma\ (P/P_0)^2$	$c/c_0 = 1 + \beta P/P_0 + \gamma\ (P/P_0)^2$
V_2AlC	47	$1 - 0.0010\ P/P_0 - 7 \times 10^{-7}\ (P/P_0)^2$	$1 - 0.0022\ P/P_0 + 2 \times 10^{-5}\ (P/P_0)^2$
VTiAlC	47	$1 - 0.0017\ P/P_0 + 10^{-5}\ (P/P_0)^2$	$1 - 0.0018\ P/P_0 + 10^{-5}\ (P/P_0)^2$
Ti_2AlC	55	$1 - 0.0011\ P/P_0 + 7 \times 10^{-7}\ (P/P_0)^2$	$1 - 0.0024\ P/P_0 + 2 \times 10^{-5}\ (P/P_0)^2$
TiNbAlC	53	$1 - 0.0015\ P/P_0 + 9 \times 10^{-6}\ (P/P_0)^2$	$1 - 0.0025\ P/P_0 + 2 \times 10^{-5}\ (P/P_0)^2$
Nb_2AlC	38	$1 - 0.0014\ P/P_0 + 3 \times 10^{-6}\ (P/P_0)^2$	$1 - 0.0014\ P/P_0 + 9 \times 10^{-6}\ (P/P_0)^2$

and V_2AlC behave in the same way, while the opposite is true for Nb_2AlC. The differences between a/a_0 and c/c_0 are greater in the case of TiNbAlC than TiVAlC.

From relative unit cell volumes, V/V_0, versus P plots (figure 2(b))—where V_0 is the unit cell volume when $P = 1$ atm—it is clear that the bulk moduli of TiNbAlC and TiVAlC are

Table 3. Relative unit cell volume changes, V/V_0, with pressure and summary of experimental bulk moduli. The pressure derivative, K_0', were assumed to be 4. All correlation coefficient values were >0.99. Also included, in the last column, the *ab initio* total energy calculation results by Sun *et al* [22, 24].

Solid	$V/V_0 = \alpha + \beta P/P_0 + \gamma\ (P/P_0)^2$	K_0 (GPa)	K_0'	K_0 (GPa)
V_2AlC	$1 - 0.0043\ P/P_0 + 2 \times 10^{-5}\ (P/P_0)^2$	201 ± 3	4.0	195
TiVAlC	$1 - 0.0050\ P/P_0 + 4 \times 10^{-5}\ (P/P_0)^2$	183 ± 3	4.0	185
Ti_2AlC	$1 - 0.0045\ P/P_0 + 2 \times 10^{-5}\ (P/P_0)^2$	186 ± 2	4.0	166
TiNbAlC	$1 - 0.0053\ P/P_0 + 4 \times 10^{-5}\ (P/P_0)^2$	181 ± 3	4.0	—
Nb_2AlC	$1 - 0.0041\ P/P_0 + 2 \times 10^{-5}\ (P/P_0)^2$	208 ± 2	4.0	205

lower than those of the end members. Least squares fit of these data yield the results listed in table 3. Fitting the same results to the Birch–Murnaghan equation [35]:

$$P = 3/2K_0[(V/V_0)^{-7/3} - (V/V_0)^{-5/3}][1 + 3/4(K_0' - 4)[(V/V_0)^{-2/3} - 1]]$$

yields K_0 values of 181 ± 2 GPa for TiNbAlC and 184 ± 3 GPa for TiVAlC. For these calculations, the pressure derivative value, K_0' was chosen to be 4. The K_0 values reported herein are in line with previous MAX phase results in that these solids are elastically quite stiff [11–16, 18, 19].

However, what is most noteworthy in this work is the solid solution *softening* effect observed. Replacing the V with Ti in V_2AlC results in a 8.5% reduction in K_0 (table 3); replacing Nb by Ti in Nb_2AlC results in a 13% reduction in K_0, which is significant. When the results shown in figure 2(a) are compared to those of Nb_2AlC (not shown) it becomes obvious that the majority of the drop in K_0 is due to a significant softening along the c-axis. (a/a_0 for Nb_2AlC is almost identical to that of TiNbAlC; c/c_0 for Nb_2AlC is slightly higher than the highest values plotted in figure 2(a).) The exact reason for this state of affairs is not entirely clear at this time, but a recent careful study of the x-ray absorption spectroscopy, EELS, and full-potential augmented plane wave study of TiNbAlC and its end members yields an important clue [33]. The major conclusion of that work was that the Nb–Ti planes are corrugated at the atomic scale. Such a corrugation is fully consistent with the greater contraction of the c-axis with pressure and the smaller contraction along the a-axis, as observed here.

Note that the alternate interpretation, viz. that the softening is due to a weakening of the bonds, is inconsistent with the fact that *both* the lattice parameters [21] and thermal expansion coefficients of the solid solution lie *in between* those of the end members. As important, the Debye–Waller factors at 10 K of *both* TiNbAlC and Nb_2AlC are significantly *lower* than those of Ti_2AlC [33]. Furthermore, given that the atomic radius of Ti (140 pm) is midway between those of V (135 pm) and Nb (145 pm) the softening observed cannot be ascribed to a size effect. Had it been a size effect, the softening would have occurred equally in TiVAlC. This comment notwithstanding, and as noted above the replacement of V by Ti in V_2AlC also results in a 8.5% reduction in K_0 and it is thus possible that some corrugation is occurring here as well. It would thus be useful to carry out a similar careful study of TiVAlC as carried out by Hug *et al* on TiNbAlC [33]. Note that without the latter study, it would have been difficult to understand the relatively high compressibility along the c-axis.

Finally, and while the agreement between our results and those deduced from recent *ab initio* calculations are decent, the agreement belies a serious problem. In the *ab initio* work [22], K_0 of Ti_2AlC is slightly underestimated, and that of TiVAlC is clearly in between the former and V_2AlC. In other words, the *ab initio* work does *not* predict the softening observed. (The *ab initio* work did not consider TiNbAlC.) The exact reasons for the discrepancy are not clear

at this time, but a number of possibilities exist. The *ab initio* work assumes the temperature is absolute zero, and the crystals are perfect, none of which are the case here. Another, more likely, reason is the limitation imposed by the calculations. It is difficult to accurately capture a random solid solution in the relatively small supercells used for the calculations. The *ab initio* work is better suited for, and a better predictor of, ordered solid solutions.

4. Conclusions

Using a synchrotron radiation source and a diamond anvil cell, we measured the pressure dependences of the lattice parameters of TiNbAlC and TiVAlC. Up to a pressure of 55 GPa, no phase transformations were observed. The bulk moduli of the solid solutions were found to be lower than those of their end members. The effect of replacing V by Ti, however, is more subtle than that of replacing Nb by Ti. In the latter case, K_0 decreases by 13%, with most of the drop taken by a softening of the *c*-axis. This effect is believed to occur because of the corrugation of the Ti–Nb planes in TiNbAlC.

Acknowledgments

This work was financially supported by a grant from the National Science Foundation (DMR 0231291) and the Division of Materials Research, NSF (DMR 0503711) to Drexel U. Part of the work was conducted at Cornell High Energy Synchrotron Source (CHESS), supported by a NSF grant and NIH/NIGMS under award DMR 0225180. HPCAT is a collaboration between the Carnegie Institution, Lawrence Livermore National Laboratory, the University of Hawaii, the University of Nevada, Las Vegas, and the Carnegie/DOE Alliance Center (CDAC). We also would like to thank Dr C S Zha of Cornell University for his assistance.

References

[1] Barsoum M W and El-Raghy T 1996 *J. Am. Ceram. Soc.* **79** 1953
[2] Barsoum M W and El-Raghy T 1999 *Metall. Mater. Trans.* **30A** 363
[3] Barsoum M W and El-Raghy T 2000 *Am. Sci.* **89** 336
[4] Barsoum M W 2000 *Prog. Solid State Chem.* **28** 201
[5] Barsoum M W and Radovic M 2004 *Encyclopedia of Materials: Science and Technology* ed R W C K H J Buschow, M C Flemings, E J Kramer, S Mahajan and P Veyssiere (Amsterdam: Elsevier)
[6] Nowotny H 1970 *Prog. Solid State Chem.* **2** 27
[7] Sundberg M *et al* 2004 *Ceram. Int.* **30** 1899
[8] Barsoum M W, Ali M and El-Raghy T 2000 *Metall. Mater. Trans.* **31A** 1857
[9] Radovic M, Ganguly A, Barsoum M W, Zhen T, Finkel P, Kalidindi S R and Lara-Curzio E 2006 *Acta Mater.* **54** 2757
[10] Zhou A G, Barsoum M W, Basu S, Kalidindi S R and El-Raghy T 2006 *Acta Mater.* **54** 1631–9
[11] Manoun B, Gulve R P, Saxena S K, Gupta S, Barsoum M W and Zha C S 2006 *Phys. Rev.* B **73** 024110
[12] Manoun B *et al* 2004 *Appl. Phys. Lett.* **84** 2799
[13] Manoun B, Saxena S K, Liermann H P, Gulve R, Hoffman E, Barsoum M W, Hug G and Zha C S 2004 *Appl. Phys. Lett.* **85** 1514
[14] Manoun B, Saxena S K and Barsoum M W 2005 *Appl. Phys. Lett.* **86** 101906
[15] Manoun B, Saxena S K, El Raghy T and Barsoum M W 2006 *Appl. Phys. Lett.* **88** 201902
[16] Onodera A *et al* 1999 *Appl. Phys. Lett.* **74** 3782
[17] Kumar R S, Rekhi S, Cornelius A L and Barsoum M W 2005 *Appl. Phys. Lett.* **86** 111904
[18] Manoun B, Zhang F X, Saxena S K, Barsoum M W and El-Raghy T 2006 *J. Phys. Chem. Solids* **67** 2091
[19] Manoun B, Yang H, Saxena S K, Ganguly A, Barsoum M W, El Bali B, Liu Z X and Lachkar M 2007 *J. Alloys Compounds* **433** 265–8
[20] Schuster J C, Nowotny H and Vaccaro C 1980 *J. Solid State Chem.* **32** 213

[21] Salama I, El-Raghy T and Barsoum M W 2002 *J. Alloys Compounds* **347** 271
[22] Sun Z M, Ahuja R and Schneider J M 2003 *Phys. Rev.* B **68** 224112
[23] Sun Z *et al* 2003 *Appl. Phys. Lett.* **83** 899
[24] Sun Z *et al* 2004 *Solid State Commun.* **129** 589
[25] Barsoum M W, Radovic M, Zhen T, Finkel P and Kalidindi S R 2005 *Phys. Rev. Lett.* **94** 085501
[26] Barsoum M W *et al* 2003 *Nat. Mater.* **2** 107
[27] Gupta S and Barsoum M W 2004 *J. Electrochem. Soc.* **151** D24–9
[28] Liermann H P, Singh A K, Manoun B, Saxena S K, Prakapenka V B and Shen G 2004 *Int. J. Ref. Met. Hard Mater.* **22** 129
[29] Liermann H P, Singh A K, Manoun B, Saxena S K and Zha C S 2005 *Int. J. Ref. Met. Hard Mater.* **23** 109–14
[30] Greene R G, Luo H and Ruoff A L 1994 *Phys. Rev. Lett.* **73** 2075
[31] Hammersley A P 1997 FIT2D: an introduction and overview *ESRF Internal Report* ESRF97HA02T
[32] Hammersley A P, Svensson S O, Hanfland M, Fitch A N and Häusermann D 1996 Two-dimensional detector software: from real detector to idealised image or two-theta scan *High Pressure Res.* **14** 235
[33] Hug G, Jaouen M and Barsoum M W 2005 *Phys. Rev.* B **71** 24105
[34] Ahuja R 2006 private communication
[35] Birch F 1978 *J. Geophys. Res.* **83** 1257